SERI/TP-252-2952
UC Category: 59a
Preprint
DE86014502

Moisture Transport in Silica Gel Packed Beds

II. Experimental Study

Ahmad A. Pesaran (SERI)
Anthony F. Mills (University of California)

August 1986

To Appear in
International Journal of
Heat and Mass Transfer

Prepared under Task No. 3022.210
FTP No. 01-540

Solar Energy Research Institute
A Division of Midwest Research Institute

1617 Cole Boulevard
Golden, Colorado 80401-3393

Prepared for the
U.S. Department of Energy
Contract No. DE-AC02-83CH10093

MOISTURE TRANSPORT IN SILICA GEL PACKED BEDS

II. EXPERIMENTAL STUDY

Ahmad A. Pesaran*
Solar Energy Research Institute
Golden, CO 80401, USA

Anthony F. Mills
School of Engineering and Applied Science
University of California
Los Angeles, CA 90024, USA

ABSTRACT

Experiments have been performed to obtain the transient response of a thin adiabatic packed bed of silica gel after a step change in inlet air conditions. Comparisons are made with predictions using a solid-side resistance model and a pseudo-gas-side controlled model and better agreement obtained with the former model. An apparent dynamic hysteresis for adsorption/desorption with microporous silica gel is clearly in evidence, which could be due to solid side effective diffusion coefficient which decreases with increasing moisture content, or to a lesser extent to a hysteresis in the adsorption isotherm itself.

---

*At the School of Engineering and Applied Science, UCLA during the course of this work.

SERI

NOMENCLATURE

a	average pore radius
A	cross section area of bed
c_l	specific heat of liquid water
$c_{p,e}$	constant pressure specific heat of humid air
c_{pl}	constant pressure specific heat of water vapor
DAR	desiccant to air ratio, $\rho_b AL/\dot{m}_G\tau$ (dimensionless)
D	total diffusivity, defined by Eq. 13
D^*	$D\tau/R^2$ (dimensionless)
D_K	Knudsen diffusion coefficient
D_S	surface diffusion coefficient
g	equilibrium isotherm, ρm_l, = g (W,T)
$g'(W)$	derivative of equilibrium isotherm, $g'(W) = \rho(\partial m_l/\partial W)_T$
h_c	convective heat transer coefficient
H_{ads}	heat of adsorption
ID	Intermediate Density (macroporous)
K_G	gas-side mass transfer coefficient
$K_{G,eff}$	effective mass transfer coefficient
L	length of bed
m_l	water vapor mass fraction (kg water/kg humid air)

SERI

NOMENCLATURE (Continued)

$\dot{m}_G$	mass flow rate of gas mixture
N_{tu}	number of transfer units, $K_G\ L/\dot{m}_G$ or $K_{G,eff}\ L/\dot{m}_G$ (dimensionless)
P	pressure
PGC	pseudo-gas-side controlled
p	perimeter of bed
r	radial coordinate in a particle
r*	r/R (dimensionless)
R	particle radius
R	H_2O gas constant
Re	Reynolds number, $2RV/\nu$ (dimensionless)
RD	Regular Density (microporous)
RH	relative humidity, P_l/P_{sat} (dimensionless)
SSR	solid-side resistance
t	time
t*	dimensionless time, t/τ (dimensionless)
T	temperature
V	superficial velocity of air
W	desiccant water content (kg water/kg dry desiccant)
z	axial distance
z*	z/L (dimensionless)

Greek

β	$\rho_p D/K_G R$ (dimensionless)
ε	porosity (dimensionless)

SERI

NOMENCLATURE (Concluded)

ν	kinematic viscosity
ρ	density of humid air
ρ_p	particle density
τ	duration of experimental run
τ_g	tortousity factor for intraparticle gas diffusion (dimensionless)
τ_s	tortousity factor for intraparticle surface diffusion (dimensionless)

Subscripts

1	water vapor
2	dry air
avg	average value
b	bed; bulk
e	surrounding humid air
eff	effective value
K	Knudsen diffusion
in	inlet value
o	initial value
out	outlet value
p	particle
S	surface diffusion
s	s-surface, in gas phase adjacent to gel particles, or dry solid phase of the bed
sat	saturation

SERI

1.0 INTRODUCTION

Part I of this series [1] reported an analytical study of the transient response of thin silica gel packed beds to a step change in inlet air humidity or temperature. Special attention was given to moisture transport within the silica gel particles since earlier investigators [2,3,4] showed that the solid-side moisture transfer resistance is generally larger than the gas-side resistance. A model which accounts for both Knudson and surface diffusion of moisture within the particles was proposed and incorporated into a simultaneous heat and mass transfer model for predicting the transient response of thin silica gel packed beds. The model is called the Solid Side Resistance (SSR) model and includes both solid- and gas-side resistances. The predictions of the SSR model were compared with predictions of the widely used Pseudo-Gas-side Controlled (PGC) model. In the PGC model the overall mass transfer from the air stream to the silica gel is represented by a gas-side coefficient which is reduced to account for solid side resistance.

Part II of this series describes an experimental program which obtained data for the evaluation of the analytical models. A bench-scale test rig was built, and adsorption and desorption experiments performed on microporous Regular Density (RD) and macroporous Intermediate Density (ID) silica gel in adiabatic thin packed beds. Section 2 describes the experimental rig, instrumentation, procedure, and test materials; Section 3 presents the results and a discussion. Section 4 presents our conclusions.

SERI

2.0 EXPERIMENTAL METHOD

2.1 *Apparatus*

A schematic of the experimental system is shown in Fig. 1. The system consists of a dryer, an air heater, a humidifier, a blower, a heat exchanger, and a desiccant bed in a test chamber. The dryer, air heater and humidifier are used to generate the desired inlet air conditions for the test chamber; the air heater is also used to regenerate the silica gel both in the test chamber and in the dryer.

The dryer used to provide dry air for step change experiments is a stainless steel cylinder 0.55 m high, and 0.19 m in diameter. A packing height of 0.42 m of 3-8 mesh RD silica gel (Davison, Grade 01) is used. A computer code [3,4,6] was used to design the dryer and for prediction of its performance. The dryer can be isolated from the system by closing valves 2 and 4.

The air heater is used to regenerate the silica gel in both the test chamber and the dryer. It is a commercial 1.5 kW electrical heater manufactured by Pacific Chromalox. It consists of two electrical heating elements contained in a well-insulated stainless steel casing. The outlet air temperature can be controlled by controlling the power supplied to the heater with an AC Variac.

The humidifier for providing humid air for the experiments is a cast acrylic cylinder 0.73 m high and 0.72 m inside diameter, packed with 1/2 inch ceramic Berl saddles. The height of the packing in the original design was 0.5 m. However, after some preliminary tests the height was reduced to 0.25 m for

better control of humidity. The packing is supported by a perforated acrylic plate. The process air enters from below and contacts with water sprayed on top of the packing. Tap water is fed to the top of the packing. The humidifier can be removed from the system by closing valves 5 and 7.

Air flow is provided by a positive displacement rotary blower manufactured by Gardner-Denver (model 2PDR) with a capacity range of 1.4×10^{-3} to 0.1 m^3/s. The blower is driven by a 3 HP, 230 VAC, 3 phase induction motor, through a belt and pulley system. The blower capacity can be changed by operating at different shaft speeds using different pulleys, and/or by varying the rate of air by-pass, i.e., controlling valve 1. Since the blower blows the air through the system, all components are under a slight pressure.

The test chamber is a 0.13 m I.D. Pyrex glass cylinder with a wall thickness of 6.5 mm. The test chamber has three sections: the main section, a top section, and a lower section. Air enters through the top, passes through a flow straightener of about 0.18 m height of Berl saddle packing to provide a uniform flow before entering the silica gel bed. The uniformity of flow was satisfactory as checked with a hot wire anemometer. The silica gel bed is supported by a copper screen, which, in turn, is supported by the lower section of the test chamber. The height of the bed is varied by adding more or less silica gel from the top of the test chamber. To approximate the adiabatic operation, the test chamber is insulated with fiberglass during testing.

The purpose of the heat exchanger is to cool the hot process air after adsorption to a dry bulb temperature in the useful range of the hygrometer

sensor used for measuring humidity. The heat exchanger consists of a copper coil welded to an aluminum cylindrical casing. Tap water is fed to the top of the coil and the process air is passed through the aluminum cylinder cocurrently with the water. The system components are connected through 1.25 inch (O.D.) galvanized pipes and 1.5 inch rubber hose connectors. The pipes are insulated for a better temperature control and to reduce heat loss during regeneration.

2.2 *Instrumentation*

The volume flow rate is determined by a calibrated Rockwell Testmeter (model No. 415). Associated air pressure and temperature measurements are made using a mercury manometer and thermocouple, respectively, to convert volume flow water rate to mass flow rate. A standard ASME orifice system with required manometer calibrated the Testmeter. The expected error in measurement of air flow rate is less than 3%.

The pressure drops across the desiccant bed, dryer and humidifier are measured using water manometers. The air temperatures upstream (at station D) and downstream (at station E) of the bed, outlet from the humidifier (at station C), and outlet from dryer (at station B) are measured using dry thermocouples made from 30 gauge (O.D. = 0.25 mm) type K, chromel-alumel wires. Chromel-alumel thermocouples were chosen because of their resistance to corrosion in water and humid air, and also for their low conductivity so as to reduce lead conduction errors. The dry thermocouples are provided with radiation shields for reduction of radiation losses and the readings corrected where appropriate. The expected error in temperature measurement is less than $0.5^{o}C$.

SERI

The relative humidity of the process air is measured using a hygrometer manufactured by Weather Measure Corp. (Model HMS-14) with a single dielectric polymer sensor with a very short response time (90% of final relative humidity in one second). The sensor of the hygrometer can be mounted at several locations (stations C, F and G) in the system for various purposes. At each mounting station a thermocouple junction is provided for measurement of temperature along with measurement of relative humidity so that the water vapor concentration can be calculated. A resistance type hygrometer manufactured by Hydrodynamics Inc. (Model 15-3001) is also used with sensors appropriate to different humidity ranges. These sensors have a slower response than the Weather Measure sensor and thus are used for measurement of uniform humidities from the dryer or humidifier to the desiccant bed. The bed outlet humidity measurement was corrected for time lag due to the distance between the bed outlet and the measuring station. The error in measurement of relative humidity is 3%. Considering other errors in measurement of temperature and total pressure the estimated error in measurement of water vapor mass fraction is less than 6%.

All thermocouple junctions are spot welded and connected to a millivolt recorder and a cold junction compensator manufactured by Fluke Company (model 2240A Datalogger). The voltage outputs of all the thermocouples and the hygrometers are recorded simultaneously at a preprogrammed time interval by the Datalogger.

2.3 *Procedure*

Tests were performed to determine the transient response of thin silica gel packed beds to a step change in inlet conditions. A bed of known initial water content and temperature was prepared using the heater of the humidifier, and then sealed. Commencing at time t=0 process air with selected constant humidity and temperature was passed through the bed. The outlet air conditions (temperature and relative humidity) from the bed were measured as a function of time and the data collected. Two types of experiments were performed, namely, adsorption and desorption. In adsorption experiments, the initial bed water content is lower than the equilibrium value corresponding to the process air, i.e., $W_o < W(m_{l,in}, T_{in}, P)$. In desorption experiments, the initial bed water content is higher than the equilibrium value corresponding to the process air, i.e., $W_o > W(m_{l,in}, T_{in}, P)$. The experiments were terminated after 20-30 minutes which is typical of cycle times between adsorption and desorption processes encountered in operation of dehumidifiers in desiccant cooling systems. The collected data were converted to engineering units and plotted and compared with the model predictions as shown in Section 3.

2.4 *Test Material*

Both microporous silica gel (Regular Density, Davison Grades 01, 03, 40 and 408) and macroporous silica gel (Intermediate Density, Davison Grade 59) were tested to investigate the effect of average pore diameter and equilibrium isotherm on bed performance. The major difference in various grades of RD gel is their range of particle size. It is reasonable to assume that the solid

side resistances varies with gel particle size and thus a wide range of gel sizes was tested (0.6-5 mm in diameter). Since the particle size range in some of the grades are wide, they were sieved to obtain a narrow range of particle size. The average pore sizes supplied by the manufacturer are 11 Å for RD gel, and 68 Å for ID gel.

3.0 RESULTS AND DISCUSSION

Thirty-five tests were performed: due to space limitations only the results of selected tests are used here to evaluate the validity of the theoretical models. Table 1 summarizes the pertinent parameters of the tests. We have presented 13 tests to show the results for two types of gel, adsorption and desorption cases, various particle sizes, and initial and inlet air conditions. The outlet air temperature and outlet water vapor mass fraction as functions of time after a step charge in inlet air conditions to the bed are shown by symbols in Figures 2 through 15 for thirteen tests. Predictions using both the solid-side (SSR) model and the pseudo-gas-side controlled (PGC) model are also shown in these figures by solid lines. For convenience the essential differences between these models are summarized in Table 2.

3.1 *Adsorption on Regular Density Silica Gel*

Figures 2 through 7 show results for adsorption tests with RD gel. The general trends of the curves for the experimental results and the theoretical predictions are similar and are explained in Part I for their series [1]. Unless otherwise specified Eq. (A-1) was used for the equilibrium isotherm and

Eq. (A-3) for the test of adsorption in the predictions. Eq. (A-6) was used for the effective surface diffusion coefficient. Since the parameter $D_{o,eff}$ had not been previously established for the H_2O-silica gel system, we determined a suitable value by making calculations for a range at $D_{o,eff}$ values and comparing predictions with experiment: Figures 3 and 4 show typical results of such predictions. Based on a number of such comparisons a value of $D_{o,eff} = 1.6 \times 10^{-6}$ m^2/s was chosen [5]. Theoretical predictions with the SSR model were not made for tests on gel particles of 0.87 mm radius and smaller: the large values of N_{tu} for these tests required a large number of time and spatial node points to avoid numerical instability and thus the computational cost was prohibitive.

By comparing predictions with experiments the following general observations can be made. Predictions of $m_{1,out}$ using the SSR model are generally superior to those of the PGC model, especially at small times. The initial slopes of the $m_{1,out}$ curves from SSR model are steeper than those of PGC model and usually match the experimental results. The PGC model usually underpredicts the experimental $m_{1,out}$, i.e., more water is adsorbed due to less mass transfer resistance. In most of the experiments the measured T_{out} is within the range of the predicted values of both SSR and PGC models; at small times the agreement with SSR model is generally better. The SSR model tends to predict peak values of T_{out} which are higher than those for PGC model with the peaks occurring earlier.

SERI

3.2 *Desorption from Regular Density Gel*

Figures 8 through 11 show results for desorption tests on RD gel. Again the theoretical predictions using both models follow the general trend of the experimental results. Again Eqs. A-1 and A-3 are used for the equilibrium isotherm and heat of adsorption, respectively. For the moisture diffusivity, Eqs. (A-5 and A-8) are used, i.e., only surface diffusion is considered for RD gel. Figures 12, 13, and 14 show that $D_{o,eff} = 0.8 \times 10^{-6}$ m^2/s gives a better match with experiment than the value of 1.6×10^{-6} used for the adsorption experiments. The lower value of $D_{o,eff}$ increases the solid side resistance and thus decreases the desorption rate: $m_{1,out}$ is overpredicted by both models (even when the reduced value of $D_{o,eff}$ is used in the SSR mode), while T_{out} is predicted satisfactorily by the SSR model, and is underpredicted by the PGC model. The prediction of $m_{1,out}$ by the PGC model matches better than that by the SSR model for Test 25 (Fig. 8), while the reverse is true for Tests 29 and 30 (Figs. 9 and 10), when $D_{o,eff} = 0.8 \times 10^{-6}$ m^2/s is used in the SSR model. A theoretical prediction for Test 35 (Fig. 11) using the SSR model was not obtained owing to a prohibitive computer cost associated with the large N_{tu} value. For this test the PGC model predicts T_{out} satisfactorily, while $m_{1,out}$ is again overpredicted. The discrepancy between predictions of the SSR and PGC models in Figures 8-10 is because they differ fundamentally as can be seen from Table 2.

It is clear that there is a fundamental difference between the behavior of the bed during adsorption and desorption. For example, the experimental responses of an adsorption test (#24) and a desorption test (#29) with similar bed and flow conditions shown in Figure 12 present this difference. As discussed in

SERI

Part I [1], the SSR model shows that there should be a difference due to concentration dependence of $D_{S,eff}$ in the Sladek theory, Eq. (A-8): initial rates of desorption should be higher than initial rates of adsorption with all other pertinent parameters the same. However a comparison of figures shows that exactly the opposite is true. Furthermore our comparison of predictions with experiments has shown that solid side effective diffusion coefficients appear to be one half of those for adsorption. The SSR model lacks an essential feature: either there is a marked hysteresis in the adsorption isotherm, or solid side effective diffusion coefficients decrease with increasing gel moisture content W. Indeed, Kruckels [1,9] found it necessary to include such a feature in correlating his experimental data for adsorption on RD gels at low moisture contents, as discussed in Part I of this series. The isotherm of RD gel usually does not show a strong hysteresis [e.g., 7 and 8]. However, decrease of solid side effective diffusion coefficient with increasing gel moisture content is quite possible. The negative exponential dependence of $D_{S,eff}$ in Eq. (A-8) is due to the decrease of heat of adsorption with increasing moisture content and has a rational basis; hence, one must look elsewhere for an explanation. A similar behavior (i.e., good agreement for adsorption and poor agreement for desorption) was observed by Barlow [10] and thus this apparent dynamic hysteresis can now be regarded as a firmly established feature of RD silica gel behavior. Further experiments are needed, in which the initial gel moisture content is varied over a wide range so as to resolve whether the apparent dynamic hysteresis is due to a gel moisture content dependent effective surface diffusion coefficient, or whether there is a more fundamental difference between the adsorption and desorption processes on a molecular scale. It should be noted than an effective porosity which decreases with increasing moisture content is not an unreasonable explanation.

SERI

3.3 *Adsorption on Intermediate Density Silica Gel*

The results for adsorption on ID gel are shown in Figures 13 through 15. Equations A-2 and A-4 were used for the equilibrium isotherm and heat of adsorption, respectively. For the moisture diffusivity Eqs. A-6, A-7 and A-8 are used, i.e., both Knudsen and surface diffusion are considered for ID gel. The $D_{o,eff}$ value used was the same as that established for adsorption on RD gel, i.e., 1.6×10^{-6} m^2/s, and a reasonable match between SSR model predictions and experiment is obtained.

The general shapes of the T_{out} and $m_{1,out}$ curves are the same as those of RD gel. However, since the equilibrium capacity of ID gel is much lower than that of RD gel (as shown in Fig. A.1), the ID gel bed loses its adsorption capacity faster. Thus, $m_{1,out}$ increases very rapidly initially and then there is a smooth transition to a more gradual increase; T_{out} also increases to its peak value very quickly, and subsequently decreases rapidly to the inlet air temperature. The predictions of $m_{1,out}$ of SSR model is better than those of PGC model, especially at small times. This behavior is similar to that noted before for adsorption experiments on RD gel. At longer times, $m_{1,out}$ is overpredicted by SSR model. Usually, the PGC model underpredicts the experimental $m_{1,out}$ initially and overpredicts later. T_{out} is generally underpredicted by both models, especially after the peak value is reached, with PGC model doing somewhat better than SSR model.

SERI

4.0 CONCLUSIONS

1. Reasonable agreement between prediction and experiment for RD gels is possible with both the solid-side resistance (SSR) model and the pseudo-gas-side controlled (PGC) model, though in general the SSR model gives the better agreement.

2. The effective surface diffusion coefficient in the SSR model required to match desorption data for RD gels is about one half of that required to match adsorption data for RD and ID gels.

3. There is an apparent dynamic hysteresis for adsorption/desorption with RD gel, which could be due a solid-side effective diffusion coefficient which decreases with increasing moisture content; a less likely possibility is a hysteresis in the adsorption isotherm itself.

4. Further experiments, in which the initial moisture content of the gel is varied over a wide range, are required to clarify the cause of the apparent hysteresis.

ACKNOWLEDGMENTS

This work was supported by a grant from the Solar Energy Research Institute/ U.S. Department of Energy, Grant No. DE-FG02-80CS84056. The Technical Monitor was T. Penney. Computer time was supplied by the Campus Computing Network of the University of California, Los Angeles. The Publication Development Branch of the Solar Energy Research Institute assisted in preparing this paper.

SERI

REFERENCES

1. Pesaran, A. A. and A. F. Mills, Moisture Transport in Silica Gel Packed Particle Beds I. Theoretical Study, *International Journal of Heat and Mass Transfer*, in press.

2. Clark, J. E., "Design and Construction of Thin, Adiabatic Desiccant Beds with Solar Air Conditioning Applications," M.S. Thesis, School of Engineering and Applied Science, University of California, Los Angeles (1979).

3. Clark, J. E., A. F. Mills and H. Buchberg, Design and Testing of Thin Adiabatic Desiccant Beds for Solar Air Conditioning Applications, *J. Solar Energy Engineering, 103*, (May 1981).

4. Pesaran, A. A., "Air Dehumidification in Packed Silica Gel Beds," M. S. Thesis, School of Engineering and Applied Science, University of California, Los Angeles (1980).

5. Pesaran, A. A., "Moisture Transport in Silica Gel Particle Beds," Ph.D. Dissertation, School of Engineering and Applied Sciences, University of California, Los Angeles (1983).

6. Nienberg, J. W. "Modeling of Desiccant Performance for Solar Desiccant-Evaporative Cooling Systems," M. S. Thesis, School of Engineering and Applied Science, University of California, Los Angeles (1977).

SERI

7. W. R. Grace and Co., Davison Silica Gel, Bulletin No. 1C-15-378; and W. R. Grace and Co., *Fluid Processing Handbook*, Baltimore, Maryland (1966).

8. Jury, S. H. and H. R. Edwards, The Silica Gel Water Vapor Sorption Therm; *Can. J. Chem. Engr. 49*, 663-666 (October 1979).

9. Kruckels, W. W., On Gradient Dependent Diffusivity, *Chem. Engs. Sci., 28*, 1565-1576 (1973).

10. Barlow, R. S., Analysis of Adsorption Process and of Desiccant Cooling Systems--A Pseudo-Steady-State Model for Coupled Heat and Mass Transfer, SERI/TR-631-1329, Solar Energy Research Institute, Golden, CO, USA (1982).

SERI

APPENDIX A. AUXILIARY DATA

Beside the information already given for K_G and h_c and in Table 2, data are required for specific heats $c_{p,e}$, c_{pl}, and c_b, heat of adsorption and equilibrium isotherm relation, and bed density, silical gel density and diffusivities. The specific heats are assumed to be independent of temperature which is a reasonable assumption for the range of temperature encountered for the application of this work, namely, solar desiccant cooling systems.

The specific heats are:

$$c_{pl} = 1884 \quad J/kg\ K$$

$$c_{p,e} = c_{pl}\, m_{l,e} + c_{p2}\,(1-m_{l,e}) = 1884\, m_{l,e} + 1005\,(1-m_{l,e}) \quad J/kg\ K$$

$$c_b = c_l\, W_{avg} + c_{silica\ gel} = 4178\, W_{avg} + 921 \quad J/kg\ K$$

Equilibrium isotherms were obtained by fitting fourth degree polynomials to the manufacturer's data [9] for Regular Density (Davison, Grades 01, 03 and 40) and Intermediate Density (Davison, Grade 59) silica gels.

$$RH = 0.0078 - 0.05759W + 24.16554\, W^2 - 124.478\, W^3 + 204.226\, W^4 \quad (A-1)$$

and for ID gel,

SERI

$$RH = 1.235\ W + 267.99\ W^2 - 3170.7\ W^3 + 10087.16\ W^4 \quad W \leq 0.07$$

$$RH = .3316 + 3.18\ W \quad W > 0.07 \tag{A-2}$$

Fig. A-1 compares the equilibrium isotherm of RD and ID silica gels. The heat of adsorption is a function of gel water content and is the summation of heat of condensation and heat of wetting. A summary of the literature on heat of adsorption of H_2O on RD silica gel is given in [4]. A recommended correlation that fits the available data for RD gel is

$$\left.\begin{aligned} H_{ads} &= 3500 - 13400\ W \quad W \leq 0.05 \\ H_{ads} &= 2950 - 1400\ W \quad W > 0.05 \end{aligned}\right\} \text{ kJ/kg water} \tag{A-3}$$

For heat of adsorption on ID gel no satisfactory data was found, thus the Clausius-Clapeyron equation

$$\ln P_{1,i} - \ln P_{1,j} = H_{ads}/R \left[\frac{1}{(T_i + 273.15)} - \frac{1}{(T_j + 273.15)}\right]$$

was applied to the equilibrium isotherm of ID silica gel. The equilibrium isotherm was replotted on the $\ln P_1$ versus $1/(T + 273.15)$ plane, where an approximate straight line for a constant gel water content was obtained. The slopes of these lines gave the average heat of adsorption at each gel water content. The following equation was fitted to the results,

$$\left.\begin{aligned} H_{ads} &= -300\ W + 2095 \quad W < 0.15 \\ H_{ads} &= 2050 \quad W \geq 0.15 \end{aligned}\right\} \text{ kJ/kg water} \tag{A-4}$$

SERI

The bulk density of RD silica gel bed is 721.1 kg/m^3, and that of ID silica gel is 400.6 kg/m^3. The particle density of RD silica gel is 1129 kg/m^3, and that of ID gel is 620 kg/m^3.

As discussed in Appendix A of Part I of this work [1] the total diffusivity D depends on only surface diffusion coefficient for microporous RD gel

$$D = D_{S,eff} \tag{A-5}$$

and depends on both surface and Knudson diffusion coefficients for macroporous ID gel

$$D = D_{S,eff} + D_K \frac{g'(W)}{\rho_p} \tag{A-6}$$

where the effective diffusion coefficients are given by

$$D_{K,eff} = \frac{\varepsilon_p}{\tau_g} 22.86 \, (T + 273.15)^{1/2} a \tag{A-7}$$

$$D_{S,eff} = D_{o,eff} \exp \left[-0.947 \, H_{ads}/(T + 273.15)\right] \tag{A-8}$$

where H_{ads} is in kJ/kg water and T in ^oC and a is pore size in meter. The particle porosity (ε_p) and gas tortousity factor (τ_g) for ID gel are 0.716 and 2.0, respectively.

Table 1. Bed and Flow Conditions for the Experiments

Test #	Gel Type	Process*	R (10^{-3} m)	L (10^{-3} m)	W_o	T_o (°C)	$m_{l,in}$	T_{in} (°C)	V (m/s)	Re	N_{tu}**	DAR	τ (s)
1	RD	AD	1.94	77.5	0.0417	23.3	0.0100	23.3	0.21	49.30	22.65	0.1285	1800
4	RD	AD	1.94	75.0	0.0410	24.2	0.0105	24.2	0.32	78.60	18.74	0.0819	1800
6	RD	AD	1.94	75.0	0.0450	22.1	0.0088	22.1	0.55	150.9	14.25	0.0547	1500
7	RD	AD	1.27	65.0	0.0410	24.7	0.0106	24.7	0.39	70.0	26.29	0.0604	1800
21	RD	AD	0.435	45.0	0.0640	20.2	0.0088	20.6	0.30	16.34	98.61	0.0554	1800
24	RD	AD	2.60	50.0	0.0668	22.6	0.0109	25.6	0.40	129.8	7.62	0.0440	1800
25	RD	DE	2.60	50.0	0.260	25.4	0.0007	25.4	0.67	218.5	6.12	0.039	1200
29	RD	DE	2.60	50.0	0.368	25.0	0.0051	23.9	0.40	131.0	7.59	0.042	1800
30	RD	DE	2.60	50.0	0.370	23.8	0.0090	23.5	0.65	205.0	6.28	0.040	1200
35	RD	DE	0.33	30.0	0.220	24.3	0.0008	24.3	0.28	11.32	101.1	0.040	1800
13	ID	AD	1.94	77.5	0.0088	23.7	0.0097	23.6	0.45	109.47	16.85	0.050	1200
14	ID	AD	1.94	77.5	0.0084	23.3	0.0074	23.3	0.18	44.0	24.70	0.0813	1860
17	ID	AD	1.94	77.5	0.005	24.4	0.0063	24.4	0.67	164.19	14.21	0.033	1200

*AD: adsorption; DE: desorption

**This value of N_{tu} is for SSR model, N_{tu} for PCC model is about 1/3.4 of this value.

Table 2. Differences Between SSR and PGC Models

Model	Solid Phase Mass Balance Equation	Parameters for Solution	Equilibrium Condition
PGC	$\frac{\partial W_{avg}}{\partial t^*} = -\frac{N_{tu}}{DAR}(m_{l,s} - m_{l,e})$	$N_{tu} = \frac{K_{G,eff}\, pL}{\dot{m}_G}$; $DAR = \frac{\rho_b AL}{\dot{m}_G \tau}$	$\rho m_{l,s} = g(W_{avg}, T_s, P)$
	Initial condition: $W_{avg}(t^*=o, z^*)=W_o$;	$K_{G,eff} = 0.704 \rho V\, Re^{-0.51}$	
	No boundary conditions	$h_c = 0.683 \rho V\, Re^{-0.51}$	
SSR	$\frac{\partial W}{\partial t^*} = \frac{1}{r^{*2}} \frac{\partial}{\partial r^*}\left(r^{*2}\, D^* \frac{\partial W}{\partial r^*}\right)$	$D^* = D\frac{\tau}{R^2}$; $\beta = \frac{D\rho_p}{K_G R}$	$\rho m_{l,s} = g[W(r^*=1), T_s, P]$
		$D = D_{S,eff} + D_{K,eff}\frac{g'(W)}{\rho_p}$	
		$K_G = 1.7\, \rho V\, Re^{-0.42}$	
		$h_c = 1.6\, \rho V\, Re^{-0.42}$	
	Initial condition: $W(t^*=o, z^*, r^*)=W_o$		
	Boundary conditions:		
	$\left.\frac{\partial W}{\partial r^*}\right\|_{r^*=0} = 0$		
	$-\beta \left.\frac{\partial W}{\partial r^*}\right\|_{r^*=1} = (m_{l,s} - m_{l,e})$		

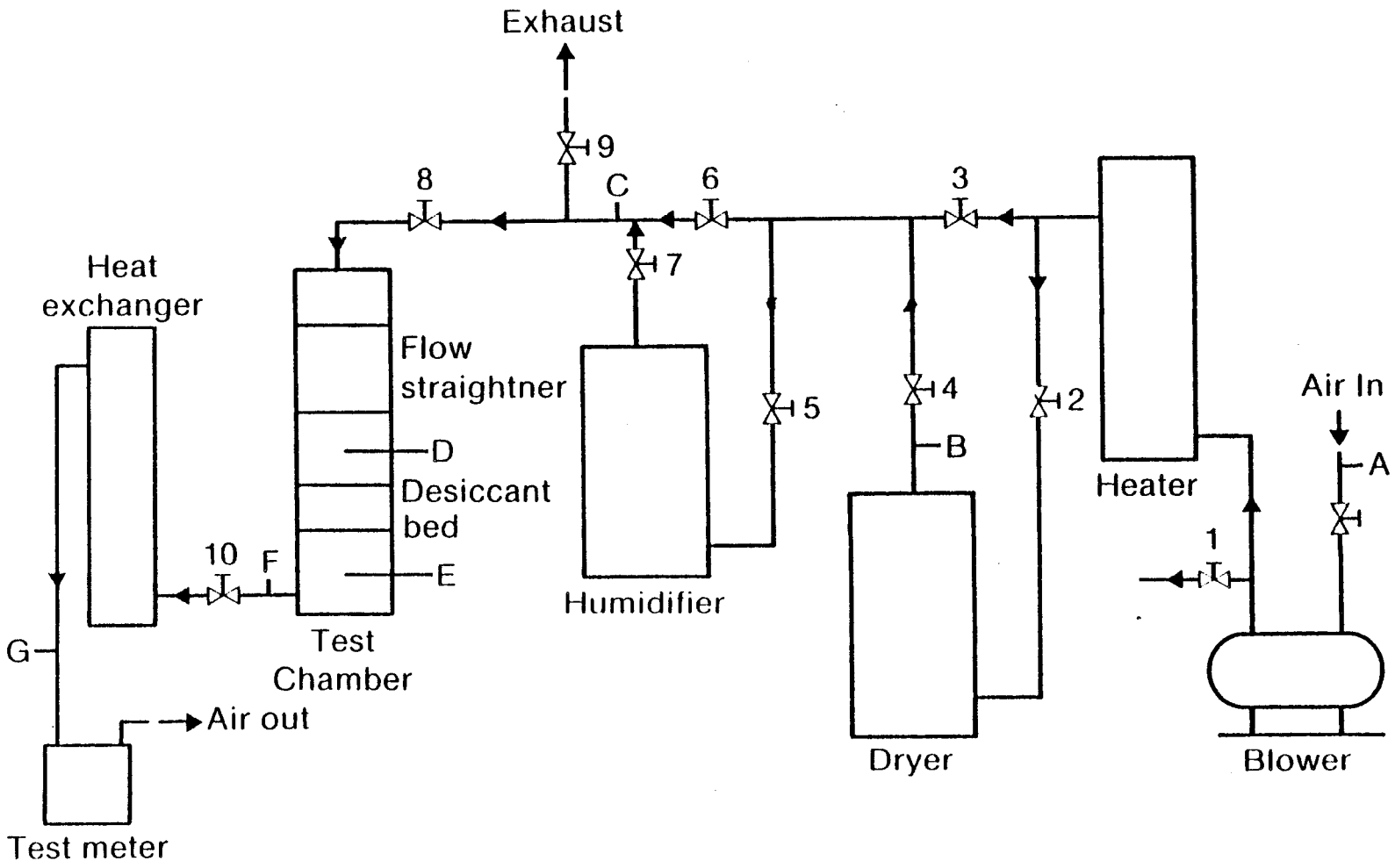

Figure 1. Experimental System Schematic

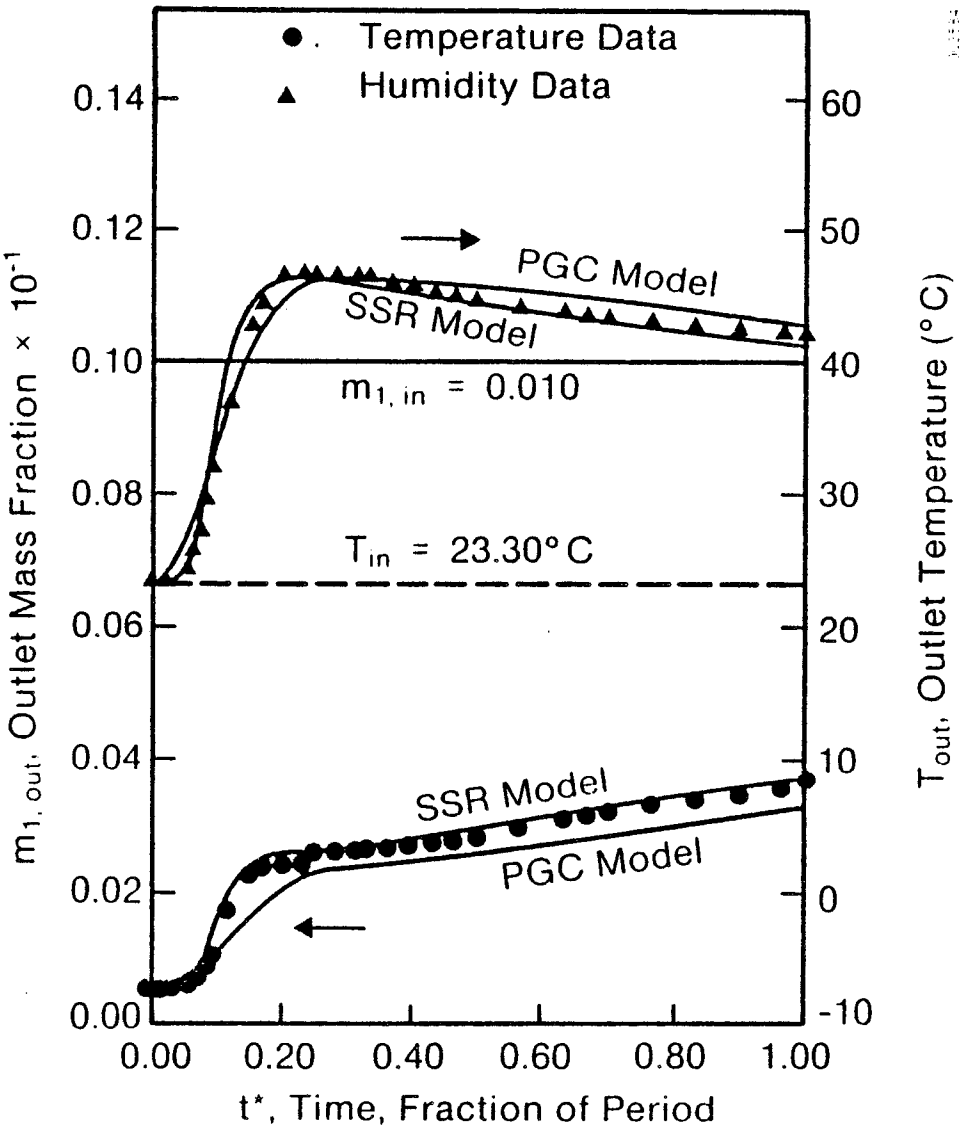

Figure 2. Comparison of Experimental and Predicted Results for Test 1

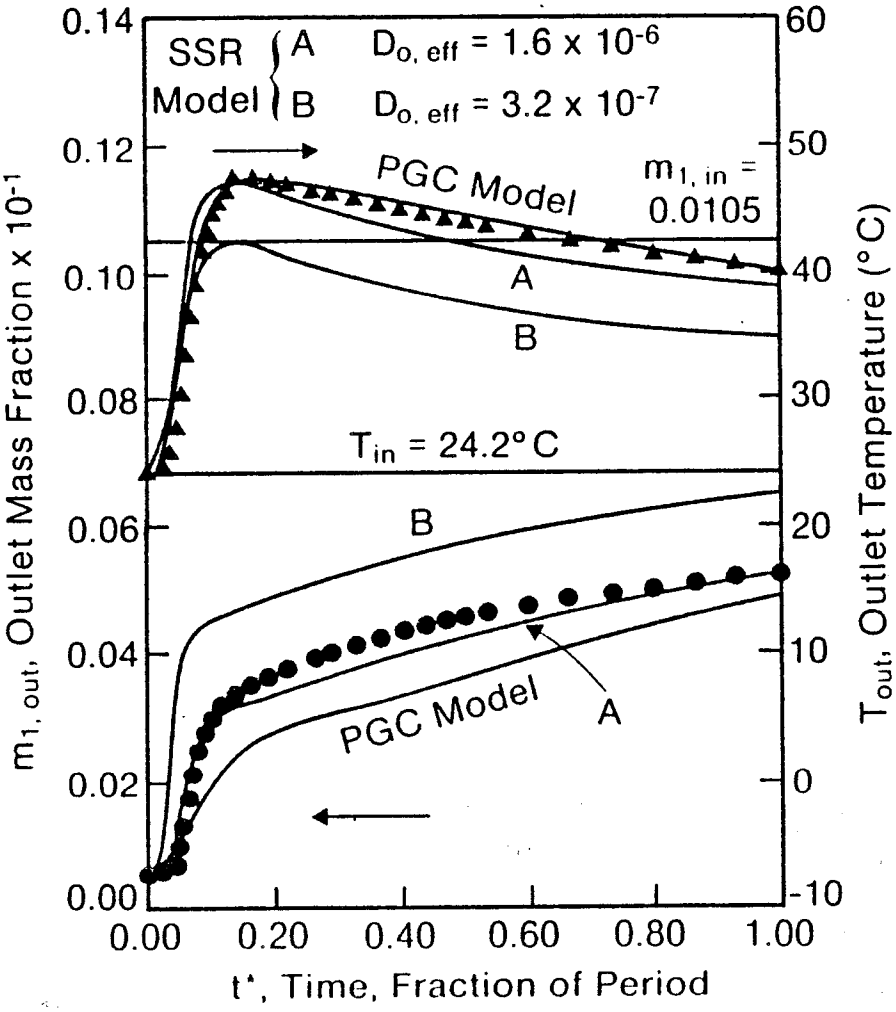

Figure 3. Comparison of Experimental and Predicted Results for Test 4; also Effect of $D_{o,eff}$

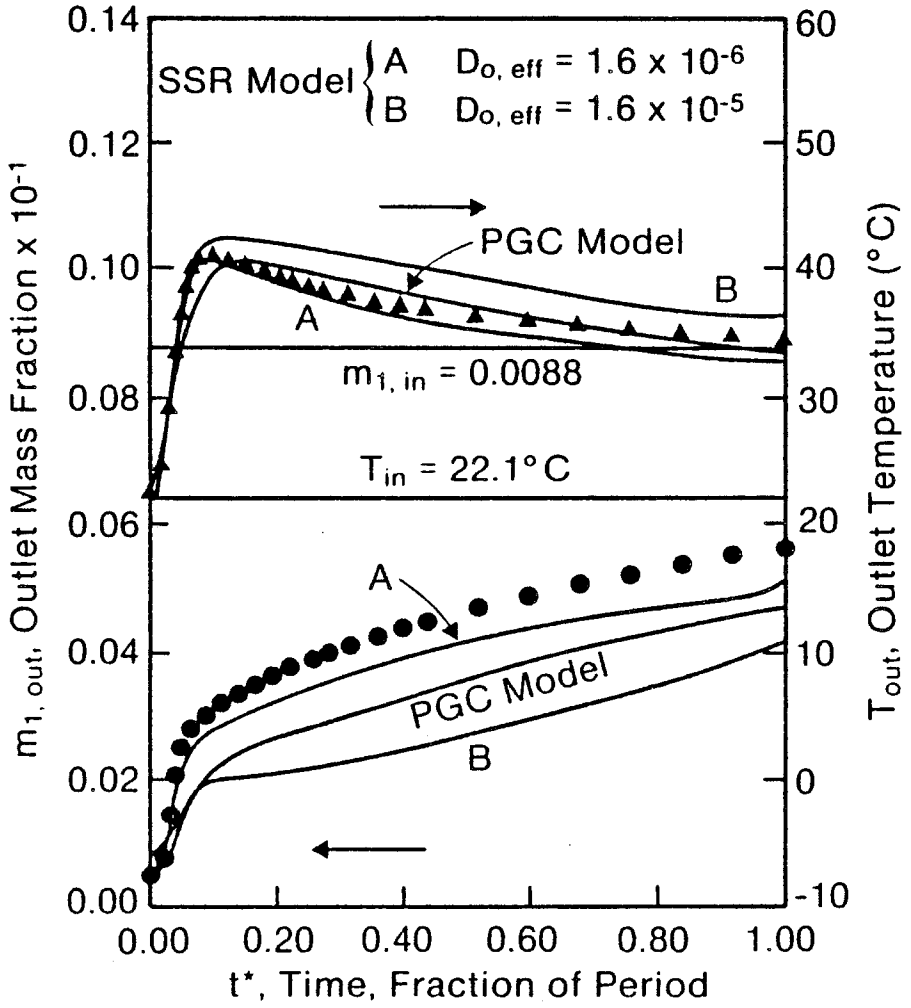

Figure 4. Comparison of Experimental and Predicted Results for Test 6; also Effect of $D_{o,eff}$

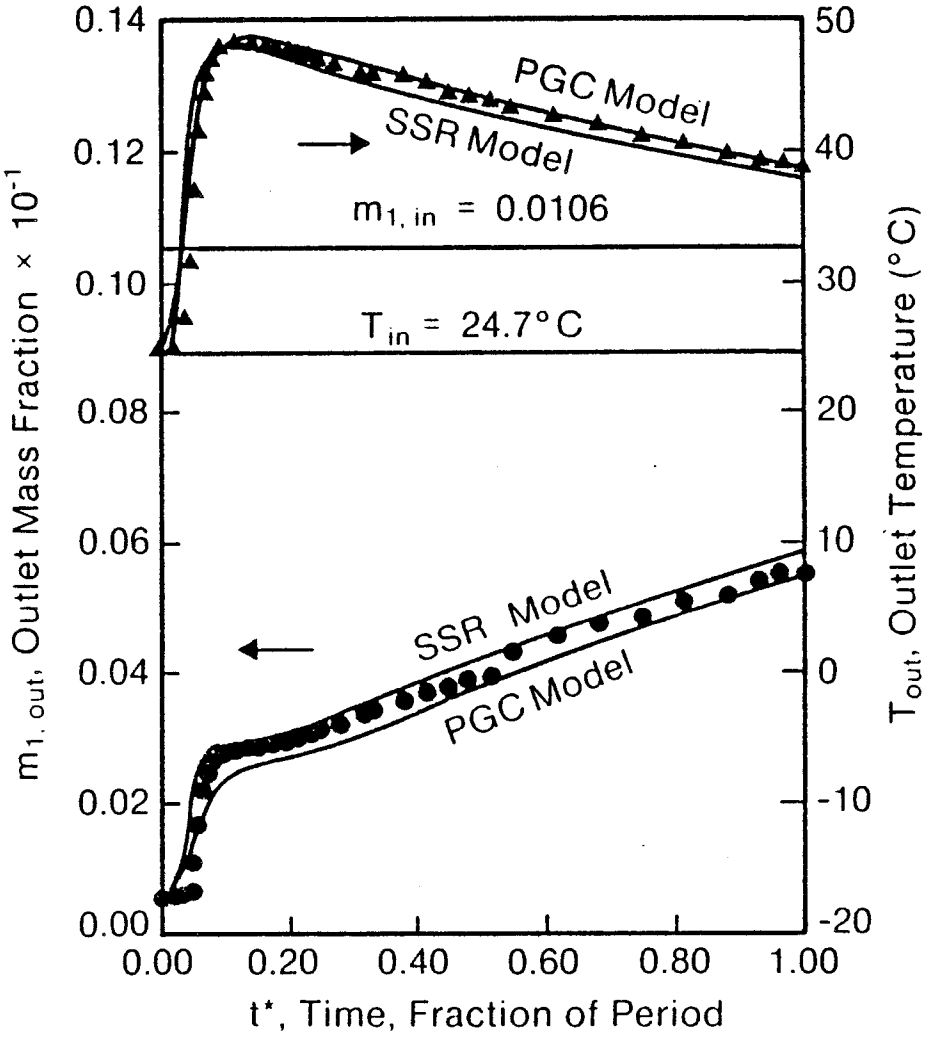

Figure 5. Comparison of Experimental and Predicted Results for Test 7

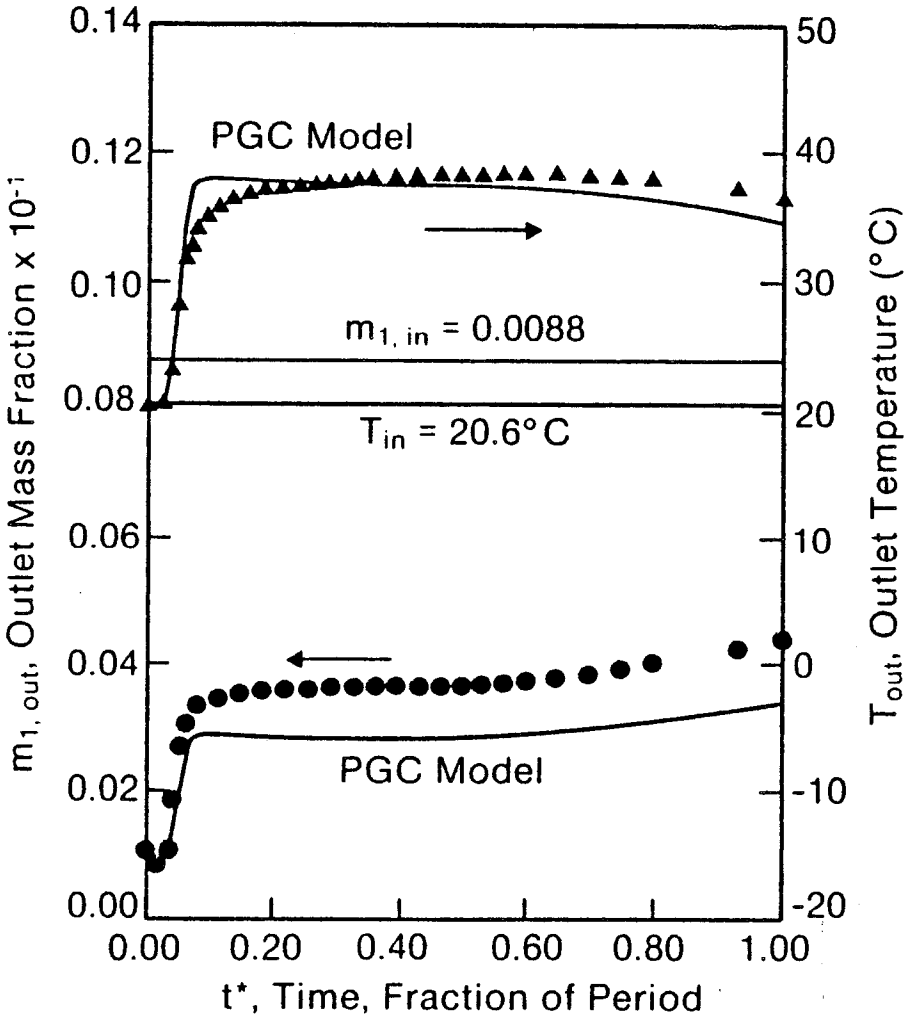

Figure 6. Comparison of Experimental and Predicted Results for Test 21

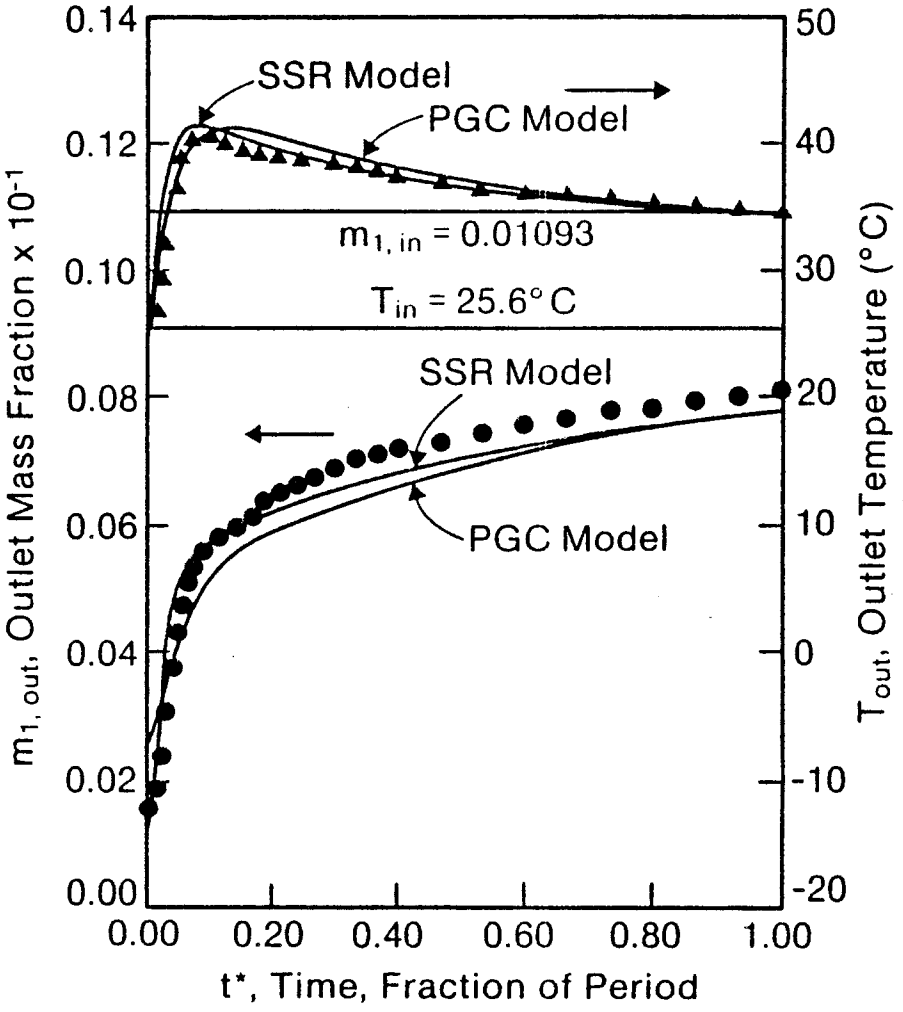

Figure 7. Comparison of Experimental and Predicted Results for Test 24

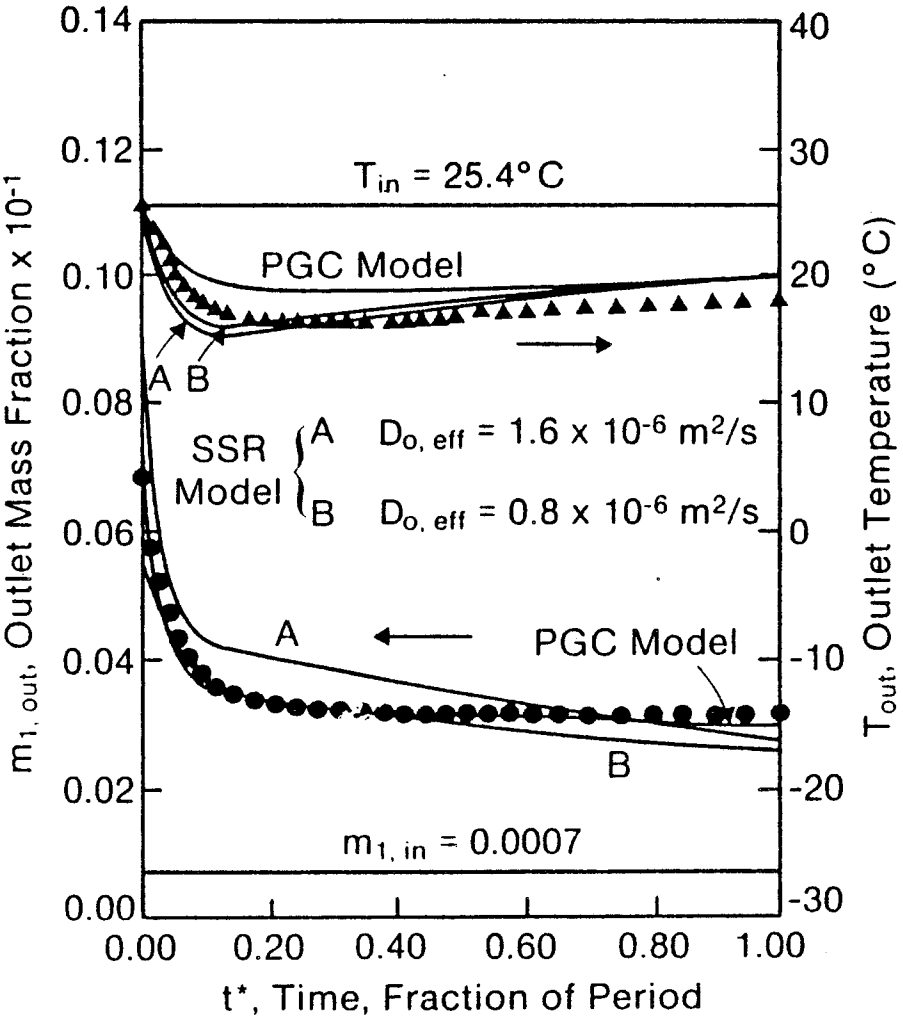

Figure 8. Comparison of Experimental and Predicted Results for Test 25

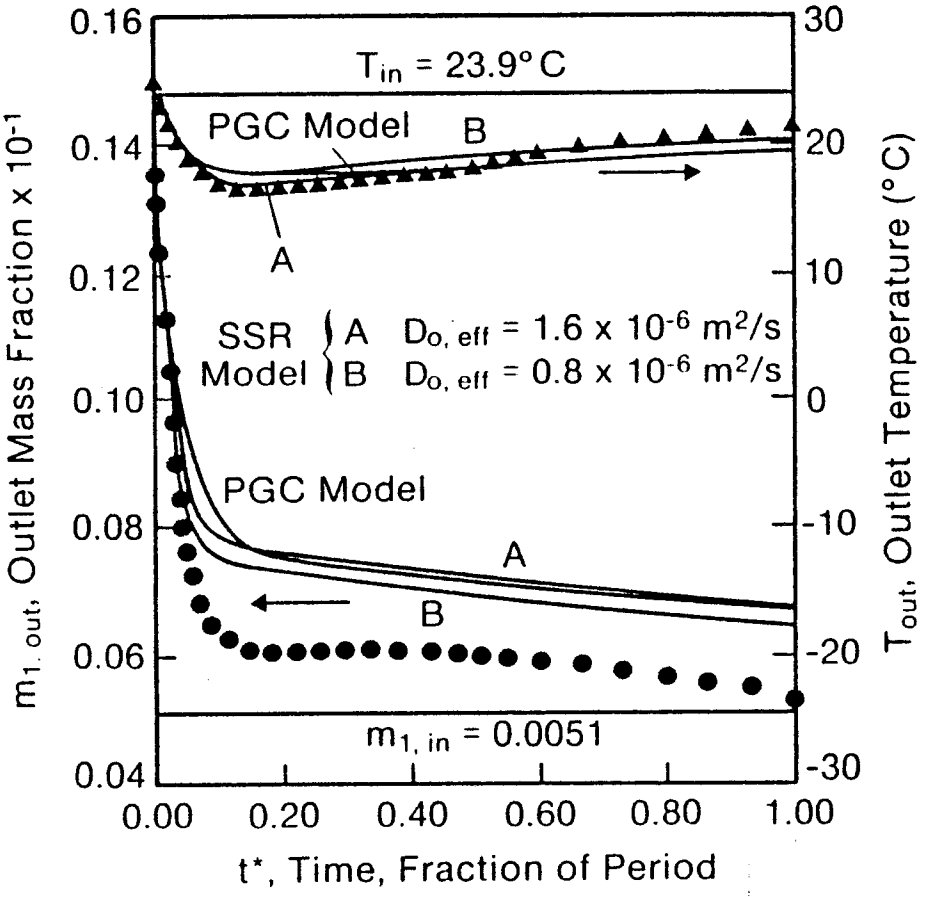

Figure 9. Comparison of Experimental and Predicted Results for Test 29

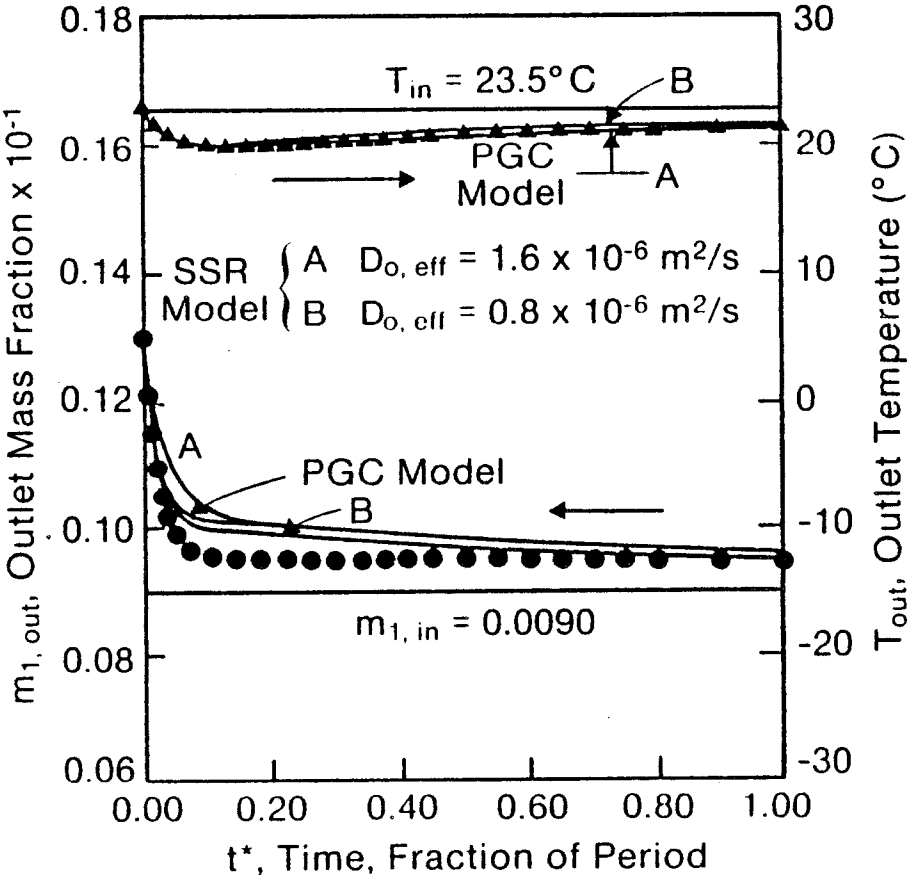

Figure 10. Comparison of Experimental and Predicted Results for Test 30

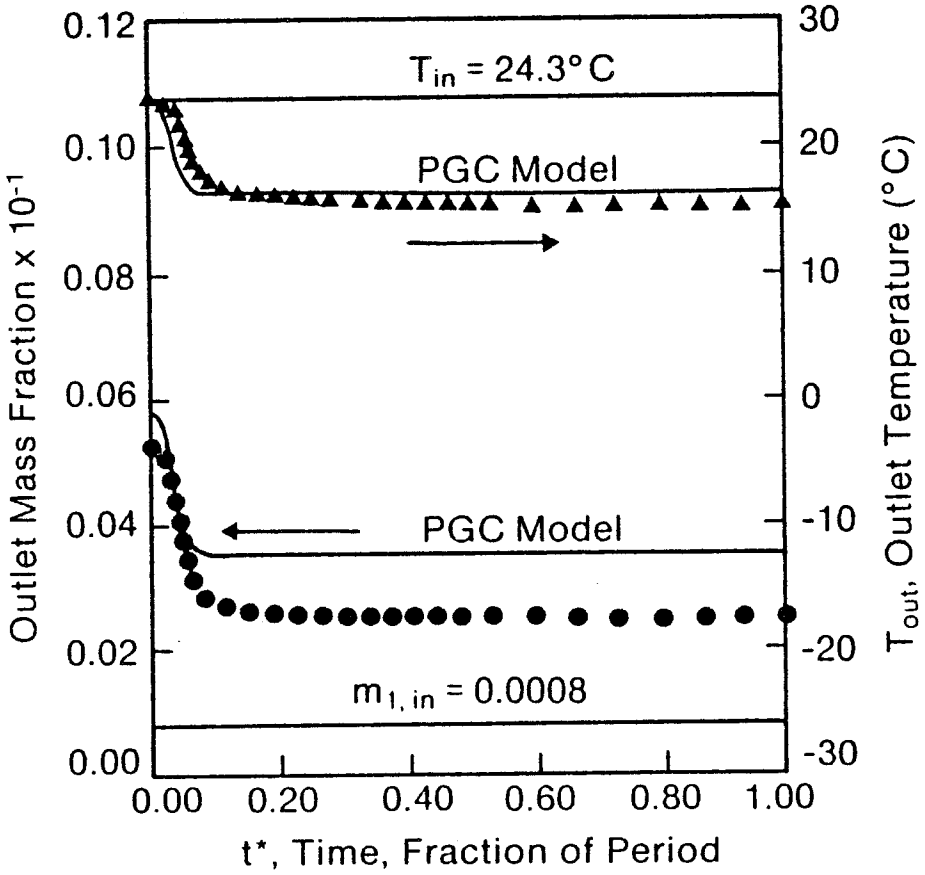

Figure 11. Comparison of Experimental and Predicted Results for Test 35

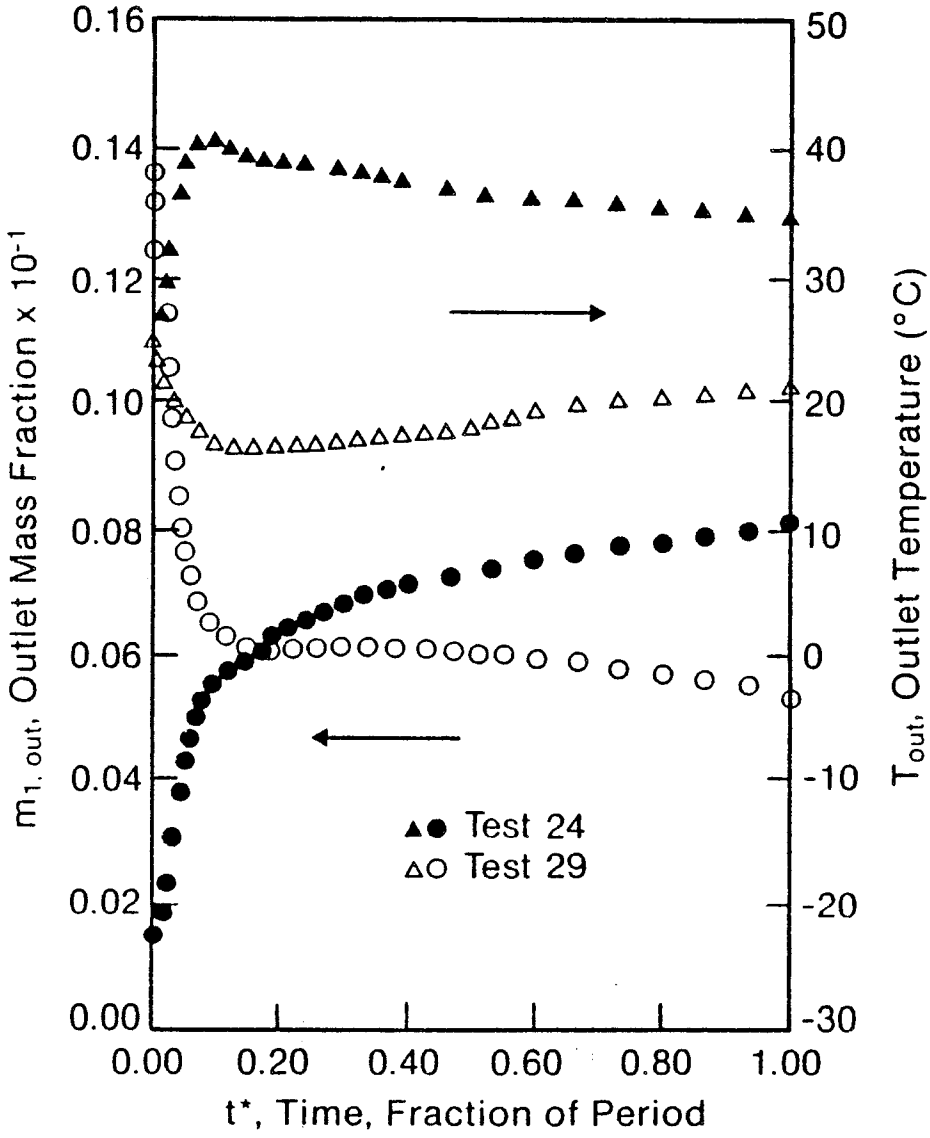

Figure 12. Comparison of an Adsorption and a Desorption Test

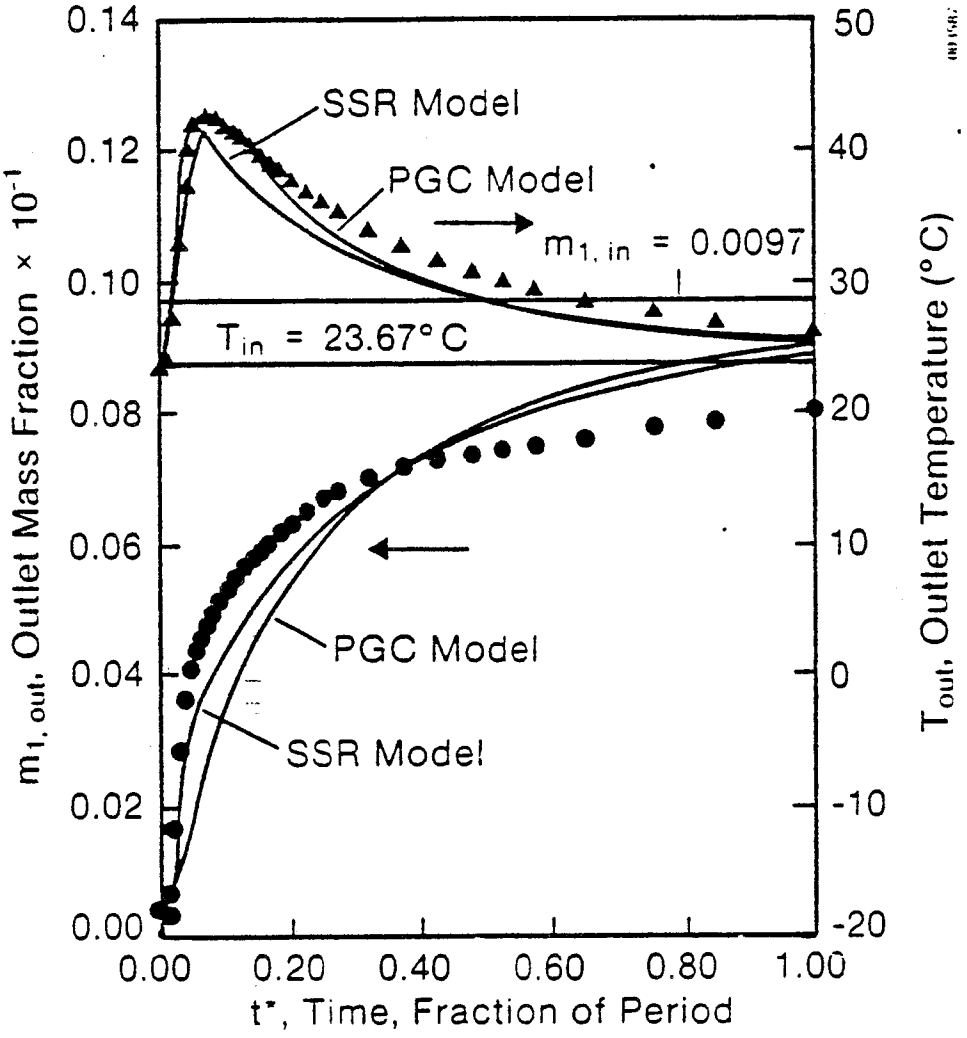

Figure 13. Comparison of Experimental and Predicted Results for Test 13

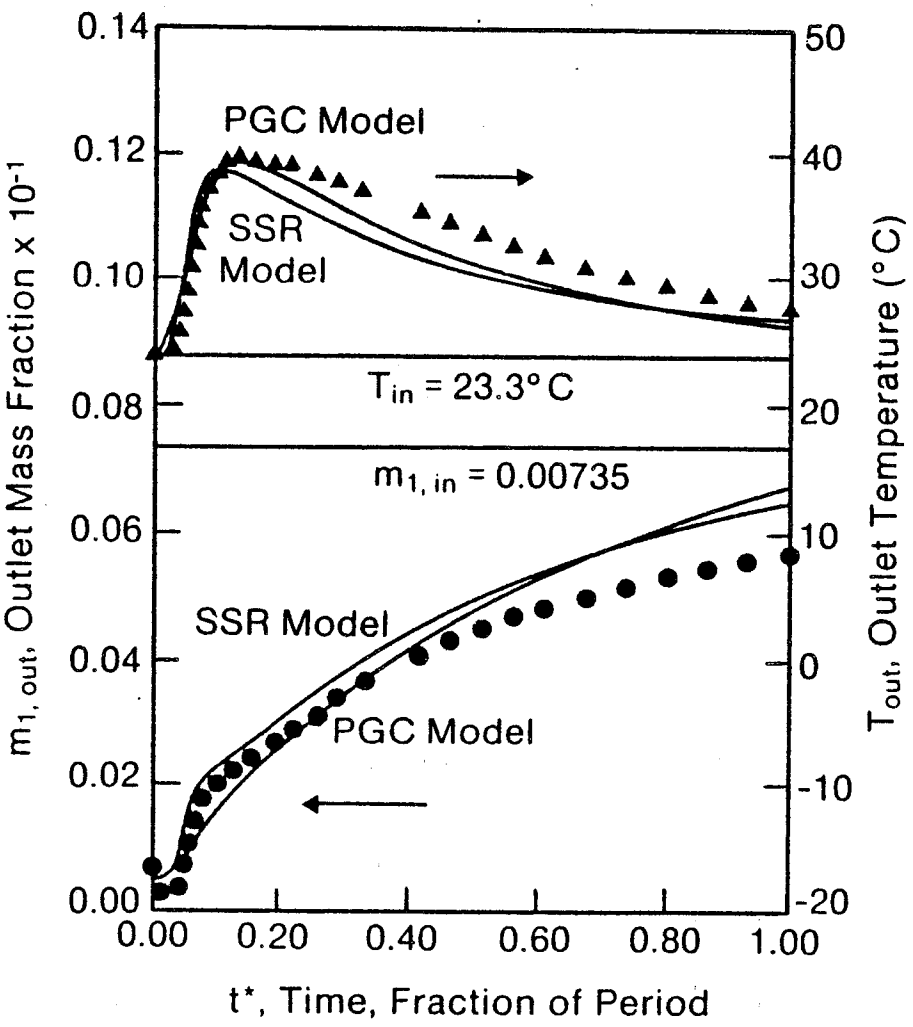

Figure 14. Comparison of Experimental and Predicted Results for Test 14

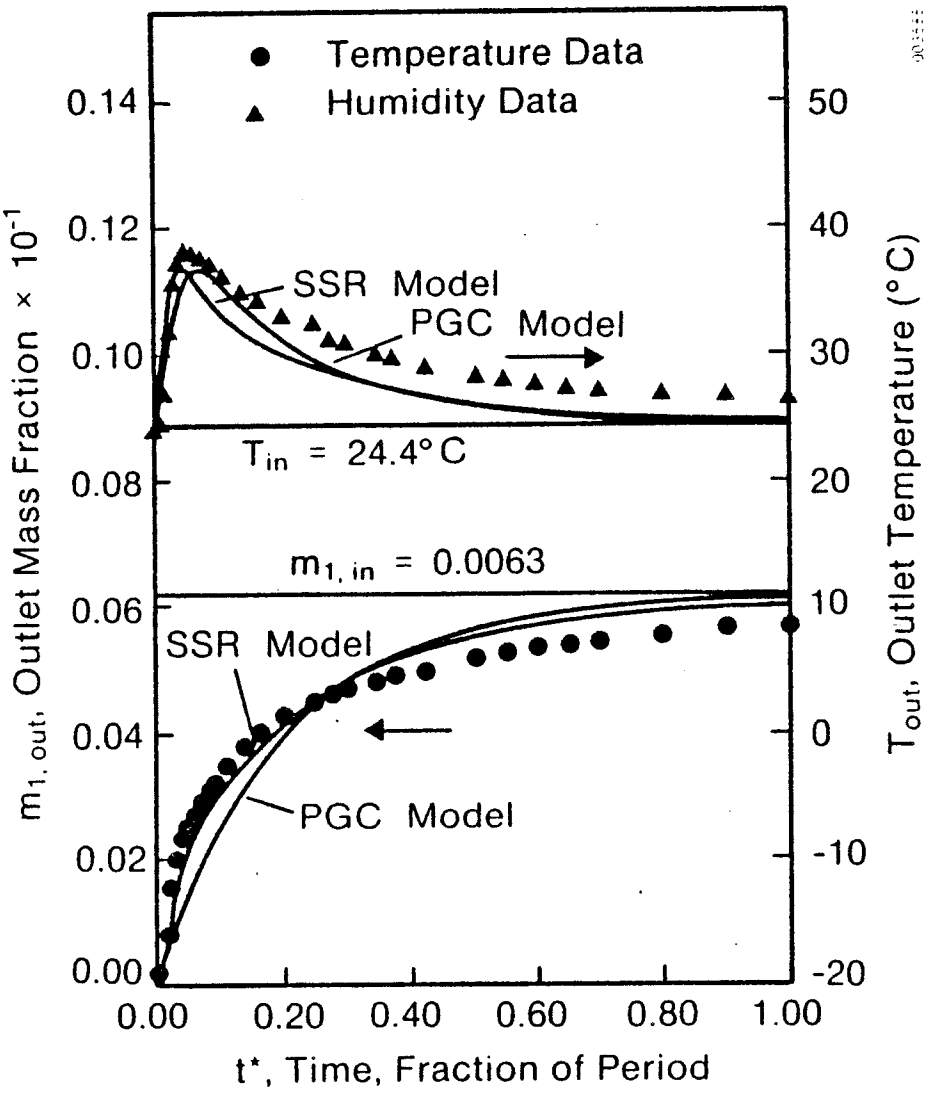

Figure 15. Comparison of Experimental and Predicted Results for Test 17

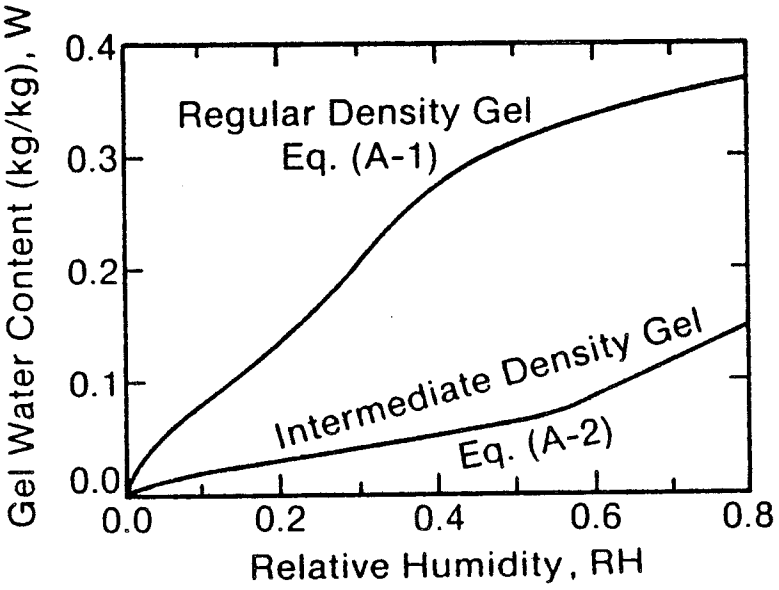

Figure A-1. Comparison of Equilibrium Isotherms of the Two Types of Silica Gel